

## A broadband terahertz quasi-optical detector utilizing lens-based antenna

GUO Da-Lu<sup>1</sup>, MOU Jin-Chao<sup>2</sup>, MA Zhao-Hui<sup>1</sup>, LI Ming-Xun<sup>1</sup>, QIAO Hai-Dong<sup>1</sup>, LV Xin<sup>1</sup>

(1. Beijing Key Laboratory of Millimeter Wave and Terahertz Technology, School of Information And Electrics, Beijing Institute of Technology, Beijing 100081, China;

2. State Key Laboratory of Millimeter Waves, City University of Hong Kong, 999077, Hong Kong)

**Abstract:** A broadband terahertz quasi-optical detector has been developed with frequency from 140 GHz to 325 GHz. The terahertz quasi-optical detector consists of a silicon lens with high resistivity and a monolithic detector chip. A double slot antenna was fabricated on the chip with a Schottky diode assembled cross the terminals of the antenna. This compact structure endows the chip with the functions of receiving THz radiations from space and converts them into baseband. To improve the directivity of the antenna on chip, the hyper-hemispherical silicon lens was designed and optimized by MLFMM (Multilevel Fast Multipole Method) algorithm, resulting in good radiation performance. The antenna gains at 220 GHz and 324 GHz was calculated to be 26 dB and 28 dB, respectively, from the measured radiation patterns. The measured responsivities of the detector achieve 1 000 ~ 4 000 V/W from 140 GHz to 325 GHz and the noise equivalent powers (NEP) were estimated to be 0.68 ~ 2.73 pW/√Hz.

**Key words:** terahertz (THz) detector, broadband, double slot antenna, silicon lens, Schottky diode

**PACS:** 07.57.Kp.

## 一种基于透镜天线的宽带太赫兹准光检波器

郭大路<sup>1</sup>, 牟进超<sup>2</sup>, 马朝辉<sup>1</sup>, 李明迅<sup>1</sup>, 乔海东<sup>1</sup>, 吕昕<sup>1</sup>

(1. 北京理工大学 信息与电子学院 毫米波与太赫兹技术北京市重点实验室, 北京 100081;

2. 香港城市大学 毫米波国家重点实验室, 香港 999077)

**摘要:**设计了一种能够工作在140~325 GHz频带的宽带准光检波器,由一颗高阻硅透镜和单片集成检波芯片组成.设计并加工出双缝天线,在天线馈电端集成了肖特基二极管,该紧凑结构使其能够接收空间中的大赫兹辐射并转换为基带信号.为增强片上天线的方向性,利用MLFMM算法进行了扩展半球硅透镜的设计和优化,实现了良好的辐射特性.通过测试,天线在220 GHz和324 GHz处的辐射增益分别为26 dB和28 dB.在140~325 GHz,检波器测试得到的响应率可达到1 000~4 000 V/W,对应的等效噪声功率(NEP)估算为0.68~2.73 pW/√Hz.

**关键词:**太赫兹(THz)检波器;宽带;双缝天线;硅透镜;肖特基二极管

中图分类号:TN454 文献标识码:A

### Introduction

The sensitivity of a detector for radiation detection is inversely proportional to the square root of its bandwidths<sup>[1]</sup>. As a result, a broadband THz detector is the key components in some imaging applications<sup>[2-3]</sup>. Com-

pared with the waveguide-based detector, which usually consists of a horn antenna and a waveguide-fed detector, the quasi-optical one can achieve wider bandwidths<sup>[4-5]</sup>. Furthermore, it is much easy to be fabricated and assembled with low cost technology. As a result, it is a good alternative for THz imaging. A broadband THz quasi-optical detector with the key device of a monolithic detector

**Received date:** 2015 - 10 - 15, **revised date:** 2016 - 04 - 01

**收稿日期:** 2015 - 10 - 15, **修回日期:** 2016 - 04 - 01

**Foundation items:** Supported by China State 863 Projects (2015AA8123012, 2015AA8125024A)

**Biography:** GUO Da-Lu (1988-), male, Shandong China. Ph. D. Research area involves terahertz device and quasi-optical component. E-mail: guodalul@bit.edu.cn

chip was designed, which have the dual functions of receiving the radiations from space and converting them into baseband. For room temperature operation, a planar Schottky diode with a surface channel was designed, which owns low parasitic effects and can detect the signals from 100 GHz to 300 GHz effectively. In addition, it can be integrated with the planar antenna easily.

The directivity of the antenna on chip, which usually has a figure-8 shaped radiation pattern, is an important factor for determining the responsivity of the detector. Because the ratio of powers radiated into the two half-spaces of the antenna with the dielectric constants of  $\epsilon_1$  and  $\epsilon_2$ , respectively, equals to  $(\epsilon_1/\epsilon_2)^{3/2}$ , the use of a substrate with high permittivity can enhance the power coupling efficiency for the on-chip antenna. For the GaAs chip, high resistivity silicon is a good choice, not only for its high relative permittivity of 11.9, but also for its low transmission loss at the frequencies between 100 GHz and 300 GHz<sup>[6]</sup>. For the silicon lens design, the aperture efficiency is focused and optimized by the multi-level fast multipole method (MLFMM). The larger the aperture efficiency is, the more the radiations will be collected under the conditions of the same physical aperture and the same radiation density.

In this letter, a broadband THz quasi-optical detector is presented, which has wide bandwidths from 140 GHz to 325 GHz with high aperture efficiency. The monolithic detector chip with a Schottky diode and a double slot antenna was designed. A hyper-hemispherical silicon lens was designed for gain enhancement and optimized for larger aperture efficiency. The quasi-optical detector was characterized. The measurement results including the radiation patterns, responsivity and noise equivalent power (NEP) are presented.

## 1 Design of the detector

Structure of the proposed detector is shown in Fig. 1. The detector is mainly composed of three parts: a silicon lens, a GaAs antenna chip and a readout circuit. All the parts are assembled into a metal shielding box, leaving the outside of the lens exposed to the space, and a K connector. The dielectric lens is caught by a fixing ring, and the antenna chip is placed on the back of the lens directly as primary source. Based on the above design, THz radiation from space is focused by the lens and received by the antenna on chip. Due to the nonlinear device (Schottky diode) embedded on the chip, the THz signals is down-converted to low frequency band or DC, which is extracted by the readout circuit. The circuit is designed of  $50\Omega$  microstrip line, and connected with GaAs chip by bonding gold wire. The whole module dimension is  $56\text{ mm} \times 38\text{ mm} \times 14\text{ mm}$ , with four arms to facilitate test. The GaAs chip is only  $500\text{ }\mu\text{m} \times 500\text{ }\mu\text{m}$ , and its micrograph is also shown in the figure 1. We give the design approach of the antenna chip and lens below.

### 1.1 Schottky diode with high cutoff frequency

The double slot antenna and planar Schottky diode was processed at the same time using sub-micro size fabrication techniques<sup>[7]</sup>. The Schottky diode operates in the thesis based on a metal and n-doped GaAs semiconductor contact structure, which has been well suited for

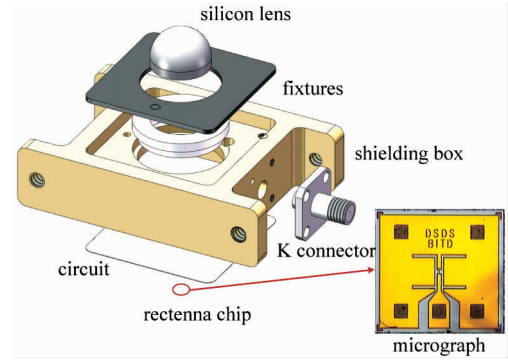


Fig. 1 Exploded view of terahertz quasi-optical detector and micrograph of antenna chip

图1 太赫兹准光探测器爆炸视图和天线芯片显微照片

high-speed applications reaching several THz. We obtained these parameters of diode through on-wafer measurement ( $I$ - $V$ ,  $C$ - $V$ ) and data fitting, as shown in Table 1. The cutoff frequency of diode was evaluated to be 2 THz above, satisfying the requirements of detecting frequency range from 140 GHz to 325 GHz.

Table 1 Parameter of the planar Schottky diode

表1 平面肖特基二极管参数

Parameters	Symbol	Unit	Value
zero offset capacitance	$C_0$	fF	$\leq 8$
series resistance	$R_s$	$\Omega$	$\leq 5$
cut-off frequency	$f_T$	THz	$\geq 2$

### 1.2 Double slot antenna with symmetrical beam

Planar double slot antenna<sup>[8-9]</sup> has symmetrical beam and well linear polarized characteristic, therefore it has

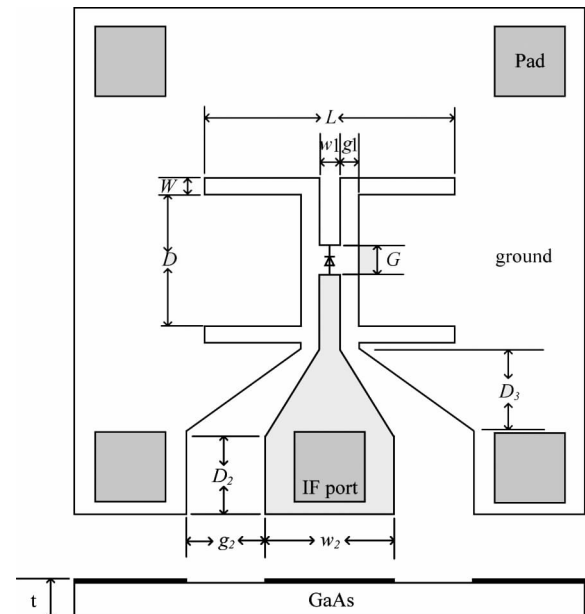


Fig. 2 The structure and parameters of planar double slot antenna in design

图2 所设计平面双缝天线的结构和参数

been used extensively in submillimeter and terahertz band. Figure 2 depicts the geometrical layout of the proposed double slot antenna. Resonant frequency of the planar antenna is determined by the slot length  $L$ , and antenna impedance is determined by slot width  $W$ . The distance of two slots  $D$  influences the coupling between them, which makes radiation pattern equal in the  $E$ - and  $H$ -plane. In the chip design, we put a Schottky diode in the middle of the two slots, and the gap length  $G$  corresponds to the diode size. IF signal can be output through a gradually changed CPW structure. On edge of the chip, it has five  $2\ \mu\text{m}$  thick pads for convenience of wire bonding.

A remarkably reduced parasitic effect of the antenna chip was obtained by thinning the substrate down to  $35\ \mu\text{m}$  through well-controlled grinding and polishing. In order to simplify the chip design complexity and achieve good matching with Schottky diode, impedance of the antenna is set to  $50\ \Omega$ . Based on process precision and simulation, the final sizes of chip are listed as table 2.

**Table 2 Design parameter of the planar double slot antenna**  
表 2 平面双缝天线设计参数

Parameters	$L$	$D$	$W$	$G$	$w_1$	$g_1$
Unit / $\mu\text{m}$	240	130	20	30	25	21
Parameters	$w_2$	$g_2$	$D_2$	$D_3$	$t$	$a$
Unit / $\mu\text{m}$	150	75	80	75	35	70

### 1.3 Dielectric lens with high gain

Despite the extra loss caused by dielectric loss and reflection, a suitable dielectric lens can focus more energy on the antenna chip. The lens can be hemispherical, ellipsoidal, or hyper-hemispherical<sup>[8-10]</sup>, etc. Hyper-hemispherical lens is a hemispherical lens with an attached extension, whose focusing effect is similar like a semi-elliptical lens. When the antenna chip is placed on the back of a dielectric lens directly as primary feed, it produces high quality Gaussian-beams<sup>[11]</sup>.

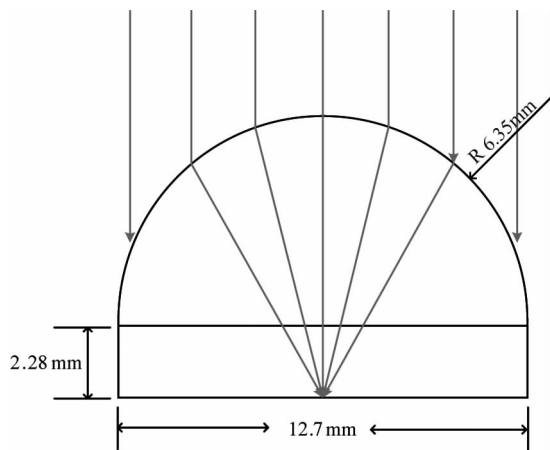


Fig. 3 Designed silicon lens model; ray tracing for the hyper-hemispherical lens structure

图 3 硅透镜模型设计, 展示超半球透镜的射线踪迹

We chose high resistance silicon ( $\rho \geq 8\ 000\ \Omega \cdot \text{m}$ ) as lens material because of its high transmission at THz

band and relative dielectric constants ( $\epsilon_r = 11.9$ ) closed to GaAs ( $\epsilon_r = 12.8$ ) to eliminate the substrate modes. The radius of the lens ( $R$ ) should ensure that the lens surface is located in the far field of the double slot antenna radiation pattern. For these purposes, we chose  $12.7\ \text{mm}$  as the lens's diameter. The extension length ( $L$ ) of the lens depends on the index of refraction of the lens used. Based on Fermat principle, we can estimate the corresponding geometric sizes and build original lens model. Then the MLFMA algorithm was applied to substitute geometrical optics method for the calculation of electromagnetic field distribution, as well as the radiation patterns computed from the established model. Finally, we gave the optimal extension length:  $L = 2.28\ \text{mm}$ . Figure 4 shows the near-field propagation of the incident wave focused by the lens, and the energy distributes approximately Gaussian field.

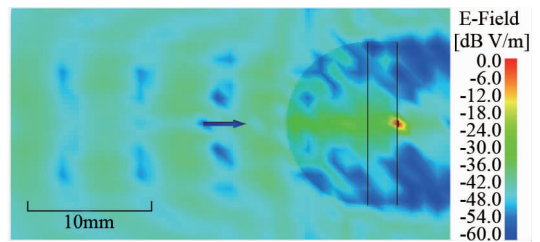


Fig. 4 Magnitude of the electric field over the near field at 320 GHz. Arrows indicates the main directions and distribution of propagation of energy

图 4 320 GHz 处近场电场幅值, 箭头代表能量传播的主方向和分布

## 2 Characterization of the detector

### 2.1 Test platform

In order to evaluate the antenna directivity and detection sensitivity<sup>[12]</sup> of the detector prototype, we utilized signal generator, amplifier/multiplier chains (VDI AMCs) and standard horns to build the quasi-optical detector test system (see Fig. 5). The output signal was collected by a spectrum analyzer. The performance analysis is depicted as follows.

### 2.2 Radiation patterns and the aperture efficiency

We chose 220 GHz and 324 GHz as the far field radiation pattern measurement frequencies. The detector under test was fixed on an electric turntable to receive the radiation (modulated at 1 MHz) from amplifier/multiplier chains. The distance between the AMCs and detector match the far-field condition ( $R \geq 2D^2/\lambda$ ,  $D$  is the diameter of lens). The diode embedded in the detector worked in the square law detection mode under small signal injection (under  $-20\ \text{dBm}$ ). The relationship between the input and output power is showed below. From the output power recorded by spectrum analyzer, we can deduce the received power of the integrated antenna, thus get the response of the antenna in various angles.

$$P_{\text{out}} = kP_{\text{in}}^2 \ (\text{mW}) \quad , \quad (1)$$

$$P_{\text{out}} = 2kP_{\text{in}} \ (\text{dBm}) \quad . \quad (2)$$

A comparison of the integrated lens antenna measurement at 220 GHz with its simulation is shown in Fig. 6

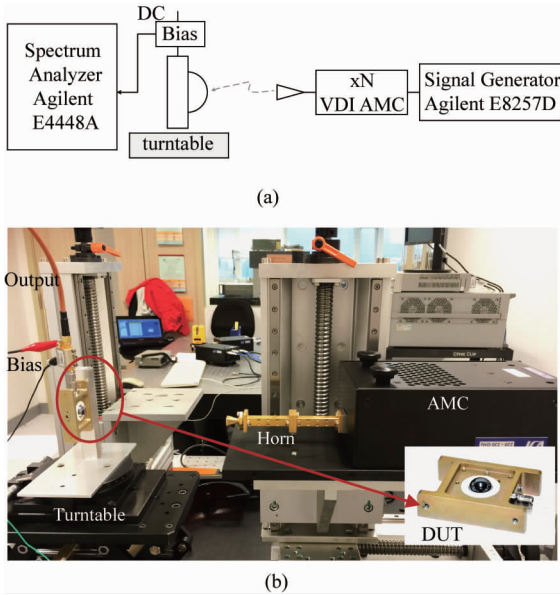


Fig. 5 (a) Block diagram of the measurement scheme, (b) Photo of the test system. Thumbnails of the detector is attached  
图5 (a) 测试方案框图, (b)测试系统照片. 附探测器实物缩略图

(a). The antenna main lobe tallies with the calculation fairly. The side lobe and back lobe is lower than expected. The straight lines appeared near  $\pm 90$  deg is due to the metal shielding box occlusion. Figure 6 (b) illustrates the similar directivity of detector at 324 GHz. Compared with low frequency, it has a narrower beam width (4.7 deg at 324 GHz vs. 6.7 deg at 220 GHz) and better radiation characteristics. Estimated antenna gain is 28 dB at 324 GHz as well as 26 dB at 220 GHz.

### 2.3 Responsivity and noise equivalent power

The antenna frequency response and diode sensitivity characteristics of the detector were estimated by the test system. The bias voltage was fixed to the optimal value 0.798V and the output power from the AMCs was set to typical mode. We used WR5.1 AMC from 140 ~ 220 GHz and WR3.4 AMC from 220 ~ 325 GHz and the average power is 4 dBm and -2 dBm, respectively. Detail of the output power is measured by PM4 power meter. The transmit horn antennas' gain  $G_T$  is 21 dB in WR-5.1 band and 25 dB in WR-3.4 band. The transmit chains and detector in the same line was adjusted to best receive location. The distance  $R$  between them is 150 mm, and the receiver antenna gain  $G_r$  has been measured above. According to the Friis transmission formula, power received by detector  $P_R$  can be figured out:

$$P_R = P_T G_T G_R \left( \frac{\lambda}{4\pi R} \right)^2 \quad (3)$$

The voltage responsivity is the ratio of the open circuit output voltage to the THz input power;  $R_{RES} = V_{OPEN} / P_R$ . The relationship between  $V_{OPEN}$  and  $P_{OUT}$  in spectrum analyzer can be expressed by  $V_{OPEN} = C \sqrt{P_{OUT}}$ . The coefficient  $C$  is calibrated to be 710 by a lock-in amplifier previously.

A frequency sweep of the measured responsivity of

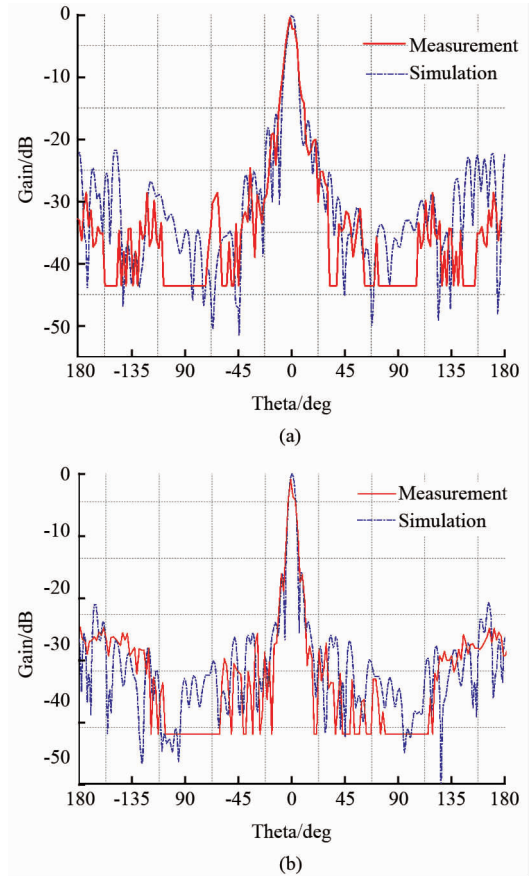


Fig. 6 Comparison of measured and simulated far-field radiation patterns of the antenna. (a) Antenna pattern at 220 GHz. (b) Antenna pattern at 325 GHz  
图6 天线远场辐射方向图测试与仿真对比 (a) 220 GHz 天线方向图, (b) 325GHz 天线方向图

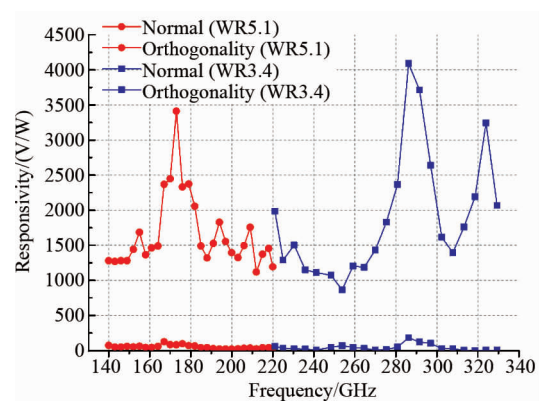


Fig. 7 Measured responsivity of the quasi-optical detector. The red and blue lines represent 140 ~ 220 GHz and 220 ~ 325 GHz, respectively. Orthogonal receiving mode is also shown in the bottom

图7 所测量准光探测器响应率. 红线和蓝线分别代表 140 ~ 220 GHz 和 220 ~ 325 GHz. 同时图底部为正交接收模式下的数值

the detector from 140 ~ 325 GHz is presented in Fig. 7. In normal receiving mode, the polarization direction of the detector is the same as transmitter, which ensures the

**Table 3 Comparisons with other reported terahertz detector****表 3 与报道的其他太赫兹检波器对比**

Frequency	Technology	Responsivity	NEP	Reference
200 GHz	Glow discharge	25 ~ 55 V/W	1 pW/√Hz	[13]
300 GHz	Schottky diode	> 100 mA/W	3 pW/√Hz	[14]
150 ~ 400 GHz	Schottky diode	300 ~ 1 800 V/W	- -	[5]
150 ~ 440 GHz	Schottky diode (ZBD)	300 ~ 1 000 V/W	5 ~ 20 pW/√Hz	[11]
100 ~ 900 GHz	Schottky diode	400 ~ 4 000 V/W	1.5 ~ 2.0 pW/√Hz	[15]
140 ~ 325 GHz	integrated Schottky diode	1 000 ~ 4 000 V/W	0.68 ~ 2.73 pW/√Hz	This work

detector to receive maximum energy. The responsivity of 1 000 ~ 4 000 V/W has been measured over frequency from 140 ~ 325 GHz. Average output power of the orthogonal receiving mode is 20 dB lower than that of normal receiving mode with corresponding responsivity from 1 ~ 10 V/W. This indicates that the designed antenna has good line polarization characteristics. From the antenna simulation and the cut-off frequency of diode, it is expected to operate on extension of frequency band, such as WR-2.8 or even higher. The noise equivalent power (NEP) of the detector can be evaluated<sup>[11]</sup> by

$$\text{NEP} \approx \frac{\sqrt{4kTB(R_s + R_d)}}{R_{\text{RES}}} \quad (4)$$

The NEP is estimated to be 0.68 ~ 2.73 pW/√Hz according to the measured data. As can be seen from table 3, the integrated quasi-detector in this work performs better than other forms of detector. The integration of design and processing of the planar antenna and Schottky diode can effectively reduce parasitic parameters and signal loss. In spite of certain disparities existed in testing method, the responsivity and NEP is superior to the reported terahertz detector.

### 3 Conclusion

A broadband terahertz quasi-optical detector based on double slot antenna chip integrated Schottky diode has been designed and fabricated. The antenna radiation pattern and responsivity of the detector was measured from 140 ~ 325 GHz at small signal levels. The introduction of large aperture silicon lens enhances the antenna gain and broadens operating bandwidth. In addition, the detector can be used as a mixer when a LO source is added with space beam splitter. Measurement at high frequency will be done with more variety of antenna chips under fabricated.

### Acknowledgement

The authors are grateful to the 13th Research Institute of China Electronics Technology Group Corporation (CECT 13), for the fabrication of GaAs chip, and State Key Laboratory of Millimeter Waves in CITYU for the

measurement.

### References

- [1] Sizov F. Photoelectronics for vision systems in invisible spectral ranges [J]. *Akadempriodika*, Kiev, 2008.
- [2] Siegel P H. Terahertz technology [J]. *IEEE Transactions on Microwave Theory and Techniques*, 2002, **50**(3): 910-928.
- [3] Dragoman D, Dragoman M. Terahertz fields and applications [J]. *Progress in Quantum Electronics*, 2004, **28**(1): 1-66.
- [4] Hesler J L, Xu H, Brissette A, *et al.* Development and characterization of THz planar Schottky diode mixers and detectors [J]. *19th International Symposium on Space Terahertz Technology*, 2008.
- [5] Hesler J L, Liu L, Xu H, *et al.* The development of quasi-optical THz detectors [C]. *IEEE IRMMW-THz*, Pasadena, 2008. 1-2.
- [6] Bolivar P H, Brucherseifer M, Rivas J G, *et al.* Measurement of the dielectric constant and loss tangent of high dielectric-constant materials at terahertz frequencies [J]. *IEEE Transactions on Microwave Theory and Techniques*, 2003, **51**(4): 1062-1066.
- [7] Mou J C, Xu M M, Chen L, *et al.* Schottky diodes with the cutoff frequency of 2.6 THz and its applications in focal imaging array [C]. *IEEE ICMMT*, 2012, **2**: 1-4.
- [8] Filipovic D F, Gearhart S S, Rebeiz G M. Double-slot antennas on extended hemispherical and elliptical silicon dielectric lenses [J]. *IEEE Transactions on Microwave Theory and Techniques*, 1993, **41**(10): 1738-1749.
- [9] Filipovic D F, Rebeiz G M. Double-slot antennas on extended hemispherical and elliptical quartz dielectric lenses [J]. *International Journal of Infrared and Millimeter Waves*, 1993, **14**(10): 1905-1924.
- [10] Huang K C, Edwards D J. *Millimetre wave antennas for gigabit wireless communications: a practical guide to design and analysis in a system context* [M]. John Wiley & Sons: UK, 2008: 145-161.
- [11] Chahal P, Morris F, Frazier G. Zero bias resonant tunnel Schottky contact diode for wide-band direct detection [J]. *Electron Device Letters*, *IEEE*, 2005, **26**: 894-896.
- [12] Liu L, Hesler J L, Xu H, *et al.* A broadband quasi-optical terahertz detector utilizing a zero bias Schottky diode [J]. *Microwave and Wireless Components Letters*, *IEEE*, 2010, **20**(9): 504-506.
- [13] Hou L, Park H, Zhang X C. Terahertz wave imaging system based on glow discharge detector [J]. *Selected Topics in Quantum Electronics*, *IEEE Journal of*, 2011, **17**(1): 177-182.
- [14] Brown E R. A system-level analysis of Schottky diodes for incoherent THz imaging arrays [J]. *Solid-State Electronics*, 2004, **48**(10): 2051-2053.
- [15] Hesler J L, Crowe T W. Responsivity and noise measurements of zero-bias Schottky diode detectors [J]. *Proc. ISSIT*, 2007: 89-92.